Journal of Mechanical Engineering Research Vol. 3(7), pp. 248-263, July 2011
Available online at http://www.academicjournals.org/jmer
ISSN 2141 - 2383 ©2011 Academic Journals

Full Length Research Paper

Comparison between the two-equation turbulence models of Jones and Launder and of Wilcox and Rubesin applied to aerospace problems

Edisson Sávio de Góes Maciel

Rua Demócrito Cavalcanti, 152, Afogados, Recife, Pernambuco- 50750-080, Brazil.
E-mail: edissonsavio@yahoo.com.br

Accepted 21st April, 2011

In the present work, the Van Leer flux vector splitting scheme is implemented on a finite-volume context. The two-dimensional Favre-averaged Navier-Stokes equations are solved using an upwind discretization on a structured mesh. The Jones and Launder and the Wilcox and Rubesin two-equation models are used in order to close the problem. The physical problems under studies are the low supersonic flow along a ramp and the moderate supersonic flow around a blunt body configuration. The implemented scheme uses a MUSCL (Monotone Upstream-centered Schemes for Conservation Laws) procedure to reach second order accuracy in space. The time integration uses a Runge-Kutta method of five stages and is second order accurate. The algorithm is accelerated to the steady state solution using a spatially variable time step. This technique has proved excellent gains in terms of convergence rate as reported in Maciel. The results have demonstrated that the Wilcox and Rubesin model has yielded more critical pressure fields than the ones due to Jones and Launder. The shock angle of the oblique shock wave in the ramp problem and the stagnation pressure ahead of the blunt body configuration are better predicted by the Wilcox and Rubesin turbulence model.

Key words: Van Leer algorithm, Jones and Launder turbulence model, Wilcox and Rubesin turbulence model, finite volumes and structured discretization, Navier-Stokes equations.

INTRODUCTION

Conventional non-upwind algorithms have been used extensively to solve a wide variety of problems (Kutler, 1975). Conventional algorithms are somewhat unreliable in the sense that for every different problem (and sometimes, every different case in the same class of problems) artificial dissipation terms must be specially tuned and judicially chosen for convergence. Also, complex problems with shocks and steep compression and expansion gradients may defy solution altogether.

Upwind schemes are in general more robust but are also more involved in their derivation and application. Some upwind schemes that have been applied to the Euler equations are: Van Leer (1982) and Radespiel and Kroll (1995). Some comments about these methods are reported as follows subsequently

Van Leer (1982) suggested an upwind scheme based on the flux vector splitting concept. This scheme considered the fact that the convective flux vector components could be written as flow Mach number polynomial functions, as main characteristic. Such polynomials presented the particularity of having the minor possible degree and the scheme had to satisfy seven basic properties to form such polynomials. This scheme was presented to the Euler equations in Cartesian coordinates and three-dimensions.

Radespiel and Kroll (1995) emphasized that the Liou and Steffen (1993) scheme had low computational complexity and low numerical diffusion when compared to other methods. They also mentioned that the original method had several deficiencies. It yielded pressure oscillations in the proximity of shock waves. Problems with adverse mesh and with flow alignment were also reported. Radespiel and Kroll (1995) proposed a hybrid flux vector splitting approach which alternated between the Liou and Steffen (1993) scheme and the Van Leer (1982) scheme, at the shock-wave regions. This strategy

assured that strength shock resolution was clear and well defined.

In relation to turbulent flow simulations, Maciel and Fico (2004) applied the Navier-Stokes equations to transonic flows problems along a convergent-divergent nozzle and around the NACA 0012 airfoil. The Baldwin and Lomax (1978) model was used to close the problem. Three algorithms were implemented: The MacCormack (1969) explicit scheme, the Pulliam and Chaussee (1981) implicit scheme and the Jameson, Schmidt and Turkel (1981) explicit scheme. The results have shown that, in general terms, the MacCormack (1969) and the Jameson et al. (1981) schemes have presented better solutions.

Maciel and Fico (2006) have performed a study involving three different turbulence models. In this paper, the Navier-Stokes equations were solved applied to the supersonic flow around a simplified configuration of the Brazilian Satellite Launcher, VLS. The algebraic models of Cebeci and Smith (1970) and of the Baldwin and Lomax (1978) and the one-equation model of Sparlat and Allmaras (1992) were used to close the problem. The algorithms of Harten (1983) and of Radespiel and Kroll (1995) were compared and presented good results.

In terms of two-equation models, Maciel and Fico (2008) have presented a work that deals with such models applied to the solution of supersonic aerospace flow problems. The 2-D Navier-Stokes equations written in conservative form, employing a finite volume formulation and a structured spatial discretization were solved. The Van Leer (1982) algorithm, first order accurate in space, was used to perform the numerical experiments. Turbulence was taken into account using two k-ε turbulence models, namely: The Jacon and Knight (1994) and the Kergaravat and Knight (1996) models. The steady state supersonic flow around a simplified version of the Brazilian Satellite Launcher, VLS, configuration was studied. The results have shown that the pressure field generated by the Kergaravat and Knight (1996) model was stronger than the respective one obtained with the Jacon and Knight (1994) model, although the latter predicts more accurate aerodynamic coefficients in this problem. The Kergaravat and Knight (1996) model predicted less intense turbulence kinetic energy- and dissipation-rate profiles than the Jacon and Knight model, yielding less intense turbulence fields.

In the present work, the Van Leer (1982) flux vector splitting scheme is implemented, on a finite-volume context. The 2-D Favre-averaged Navier-Stokes equations are solved using an upwind discretization on a structured mesh. The Jones and Launder (1972) k-ε and the Wilcox and Rubesin (1980) k-ω^2 two-equation models are used in order to close the problem. The physical problems under studies are the low supersonic flow along a ramp and the moderate supersonic flow around a blunt body configuration. The implemented scheme uses a MUSCL procedure to reach second order accuracy in space. The time integration uses a Runge-Kutta method of five stages and is second order accurate. The algorithm is accelerated to the steady state solution using a spatially variable time step. This technique has proved excellent gains in terms of convergence rate as reported in Maciel (2005, 2008).

The results have demonstrated that the Wilcox and Rubesin (1980) model have yielded more critical pressure fields than the ones due to Jones and Launder (1972). The shock angle of the oblique shock wave in the ramp problem and the stagnation pressure ahead of the blunt body configuration are better predicted by the Wilcox and Rubesin (1980) turbulence model.

NAVIER-STOKES EQUATIONS

The 2-D flow is modeled by the Navier-Stokes equations, which express the conservation of mass and energy as well as the momentum variation of a viscous, heat conducting and compressible media, in the absence of external forces. The integral form of these equations may be represented by:

$$\partial/\partial t \int_V Q dV + \int_S \left[(E_e - E_v) n_x + (F_e - F_v) n_y \right] dS + \int_V G dV = 0 \quad , \qquad (1)$$

where Q is written for a Cartesian system, V is the cell volume, n_x and n_y are components of the unity vector normal to the cell boundary, S is the flux area, E_e and F_e are the components of the convective, or Euler, flux vector, E_v and F_v are the components of the viscous, or diffusive, flux vector and G is the source term of the two-equation models.

The vectors Q, E_e, F_e, E_v and F_v are, incorporating a k-ε or k-ω^2 formulation, represented by:

$$Q = \begin{Bmatrix} \rho \\ \rho u \\ \rho v \\ e \\ \rho k \\ \rho s \end{Bmatrix}, E_e = \begin{Bmatrix} \rho u \\ \rho u^2 + p \\ \rho uv \\ (e+p)u \\ \rho ku \\ \rho su \end{Bmatrix}, F_e = \begin{Bmatrix} \rho v \\ \rho uv \\ \rho v^2 + p \\ (e+p)v \\ \rho kv \\ \rho sv \end{Bmatrix}, E_v = \begin{Bmatrix} 0 \\ t_{xx} + \tau_{xx} \\ t_{xy} + \tau_{xy} \\ f_x \\ \alpha_x \\ \beta_x \end{Bmatrix}, F_v = \begin{Bmatrix} 0 \\ t_{xy} + \tau_{xy} \\ t_{yy} + \tau_{yy} \\ f_y \\ \alpha_y \\ \beta_y \end{Bmatrix}$$

and

$$G = \begin{Bmatrix} 0 \\ 0 \\ 0 \\ 0 \\ G_k \\ G_s \end{Bmatrix} ; \qquad (2)$$

where the components of the viscous stress tensor are defined as:

$$t_{xx} = [2\mu_M \partial u/\partial x - 2/3\,\mu_M(\partial u/\partial x + \partial v/\partial y)]/\mathbf{Re},$$
$$t_{xy} = \mu_M(\partial u/\partial y + \partial v/\partial x)/\mathbf{Re}; \quad (3)$$

$$t_{yy} = [2\mu_M(\partial v/\partial y) - 2/3\,\mu_M(\partial u/\partial x + \partial v/\partial y)]/\mathbf{Re}. \quad (4)$$

The components of the turbulent stress tensor (Reynolds stress tensor) are described by the following expressions:

$$\tau_{xx} = [2\mu_T \partial u/\partial x - 2/3\,\mu_T (\partial u/\partial x + \partial v/\partial y)]/\mathbf{Re} - 2/3\,\rho k,$$
$$\tau_{xy} = \mu_T(\partial u/\partial y + \partial v/\partial x)/\mathbf{Re}; \quad (5)$$

$$\tau_{yy} = [2\mu_T \partial v/\partial y - 2/3\,\mu_T (\partial u/\partial x + \partial v/\partial y)]/\mathbf{Re} - 2/3\,\rho k. \quad (6)$$

Expressions to f_x and f_y are given as:

$$f_x = (t_{xx} + \tau_{xx})u + (t_{xy} + \tau_{xy})v - q_x$$

and

$$f_y = (t_{xy} + \tau_{xy})u + (t_{yy} + \tau_{yy})v - q_y, \quad (7)$$

where q_x and q_y are the Fourier heat flux components and are given by:

$$q_x = -\gamma/\mathbf{Re}(\mu_M/\mathbf{Pr}_L + \mu_T/\mathbf{Pr}_T)\partial e_i/\partial x$$

and

$$q_y = -\gamma/\mathbf{Re}(\mu_M/\mathbf{Pr}_L + \mu_T/\mathbf{Pr}_T)\partial e_i/\partial y. \quad (8)$$

The diffusion terms related to the k-ε or k-ω^2 equations are defined as:

$$\alpha_x = 1/\mathbf{Re}(\mu_M + \mu_T/\sigma_k)\partial k/\partial x$$

and

$$\alpha_y = 1/\mathbf{Re}\,(\mu_M + \mu_T/\sigma_k)\partial k/\partial y; \quad (9)$$

$$\beta_x = 1/\mathbf{Re}(\mu_M + \mu_T/\sigma_s)\partial s/\partial x$$

and

$$\beta_y = 1/\mathbf{Re}(\mu_M + \mu_T/\sigma_s)\partial s/\partial y. \quad (10)$$

In the aforementioned equations, ρ is the fluid density; u and v are Cartesian components of the velocity vector in the x and y directions, respectively; e is the total energy per unit volume; p is the static pressure; k is the turbulence kinetic energy; s is the second turbulent variable, which can be the rate of dissipation of the turbulence kinetic energy (k-ε model) or the square of the flow vorticity (k-ω^2 model); the t's are viscous stress components; τ's are the Reynolds stress components; the q's are the Fourier heat flux components; G_k takes into account the production and the dissipation terms of k; G_s takes into account the production and the dissipation terms of s; μ_M and μ_T are the molecular and the turbulent viscosities, respectively; Pr_L and Pr_T are the laminar and the turbulent Prandtl numbers, respectively; σ_k and σ_s are turbulence coefficients; γ is the ratio of specific heats; Re is the laminar Reynolds number, defined by:

$$\mathbf{Re} = \rho V_{REF} l_{REF}/\mu_M, \quad (11)$$

where V_{REF} is a characteristic flow velocity and l_{REF} is a configuration characteristic length.

The internal energy of the fluid, e_i, is defined as:

$$e_i = e/\rho - 0.5(u^2 + \mathbf{v}^2). \quad (12)$$

The molecular viscosity is estimated by the empiric Sutherland formula:

$$\mu_M = bT^{1/2}/(1 + S/T), \quad (13)$$

where T is the absolute temperature (K), b = 1.458 × 10^{-6} Kg/(m.s.$K^{1/2}$) and S = 110.4 K, to the atmospheric air in the standard atmospheric conditions (Fox and McDonald, 1988).

The Navier-Stokes equations are nondimensionalized in relation to the freestream density, ρ_∞, the freestream speed of sound, a_∞, and the freestream molecular viscosity, μ_∞. The system is closed by the stated equation for a perfect gas:

$$p = (\gamma - 1)[e - 0.5\rho(u^2 + v^2) - \rho k], \quad (14)$$

Considering the ideal gas hypothesis. The total enthalpy is given by $H = (e + p)/\rho$.

NUMERICAL ALGORITHM – VAN LEER (1982) SCHEME

The space approximation of the integral Equation (1) yields an ordinary differential equation system given by:

$$V_{i,j}\, dQ_{i,j}/dt = -R_{i,j}, \qquad (15)$$

with $R_{i,j}$ representing the net flux (residual) of the conservation of mass, conservation of momentum and conservation of energy in the volume $V_{i,j}$.

The residual is calculated as:

$$R_{i,j} = R_{i,j-1/2} + R_{i+1/2,j} + R_{i,j+1/2} + R_{i-1/2,j}, \qquad (16)$$

with $R_{i+1/2,j} = R^{c}_{i+1/2,j} - R^{d}_{i+1/2,j}$, where the superscripts "c" and "d" are related to convective and diffusive contributions, respectively.

The cell volume is given by:

$$V_{i,j} = 0.5\left|\left(x_{i,j} - x_{i+1,j}\right)y_{i+1,j+1} + \left(x_{i+1,j} - x_{i+1,j+1}\right)y_{i,j} + \left(x_{i+1,j+1} - x_{i,j}\right)y_{i+1,j}\right| + 0.5\left|\left(x_{i,i} - x_{i+1,i+1}\right)y_{i,i+1} + \left(x_{i+1,j+1} - x_{i,i+1}\right)y_{i,j} + \left(x_{i,j+1} - x_{i,j}\right)y_{i+1,j+1}\right| \qquad (17)$$

The convective discrete flux calculated by the AUSM scheme (Advection Upstream Splitting Method) can be understood as a sum of the arithmetical average between the right (R) and the left (L) states of the cell face (i+½,j), involving volumes (i+1,j) and (i,j), respectively, multiplied by the interface Mach number, plus a scalar dissipative term, as shown in Liou and Steffen (1993). Hence,

$$R_{i+1/2,j} = \left|S\right|_{i+1/2,j}\left(\frac{1}{2}M_{i+1/2,j}\left(\begin{bmatrix}\rho a\\ \rho au\\ \rho av\\ \rho aH\\ \rho ak\\ \rho as\end{bmatrix}_{L} + \begin{bmatrix}\rho a\\ \rho au\\ \rho av\\ \rho aH\\ \rho ak\\ \rho as\end{bmatrix}_{R}\right) - \frac{1}{2}\phi_{i+1/2,j}\left(\begin{bmatrix}\rho a\\ \rho au\\ \rho av\\ \rho aH\\ \rho ak\\ \rho as\end{bmatrix}_{R} - \begin{bmatrix}\rho a\\ \rho au\\ \rho av\\ \rho aH\\ \rho ak\\ \rho as\end{bmatrix}_{L}\right)\right) + \begin{bmatrix}0\\ S_x p\\ S_y p\\ 0\\ 0\\ 0\end{bmatrix}_{i+1/2,j}, \qquad (18)$$

where $S_{i+1/2,j} = \left[S_x \quad S_y\right]^{t}_{i+1/2,j}$ defines the normal area vector for the surface (i+½,j). The normal area components S_x and S_y to each flux interface are given in Table 1. Figure 1 exhibits the computational cell adopted for the simulations, as well its respective nodes and flux interfaces. The quantity "a" represents the speed of sound, which is defined as:

$$a = \left(\gamma p/\rho - k\right)^{0.5}. \qquad (19)$$

$M_{i+½,j}$ defines the advective Mach number at the (i+½,j) face, which is calculated according to Liou and Steffen (1993):

$$M_{i+1/2,j} = M^{+}_{L} + M^{-}_{R}, \qquad (20)$$

where the separated Mach numbers are defined by Van Leer (1982):

$$M^{+} = \begin{cases} M, & \text{if } M \geq 1;\\ 0.25\left(M+1\right)^2, & \text{if } \left|M\right| < 1;\\ 0, & \text{if } M \leq -1; \end{cases}$$

and

$$M^{-} = \begin{cases} 0, & \text{if } M \geq 1;\\ -0.25\left(M-1\right)^2, & \text{if } \left|M\right| < 1;\\ M, & \text{if } M \leq -1. \end{cases} \qquad (21)$$

M_L and M_R represent the Mach numbers associated with the left and the right states, respectively. The advection Mach number is defined by:

$$M = \left(S_x u + S_y v\right)/\left(a\left|S\right|\right) \qquad (22)$$

Table 1. Values of S_x and S_y.

Surface	S_x	S_y
i,j-1/2	$(y_{i+1,j} - y_{i,j})$	$(x_{i,j} - x_{i+1,j})$
i+1/2,j	$(y_{i+1,j+1} - y_{i+1,j})$	$(x_{i+1,j} - x_{i+1,j+1})$
i,j+1/2	$(y_{i,j+1} - y_{i+1,j+1})$	$(x_{i+1,j+1} - x_{i,j+1})$
i-1/2,j	$(y_{i,j} - y_{i,j+1})$	$(x_{i,j+1} - x_{i,j})$

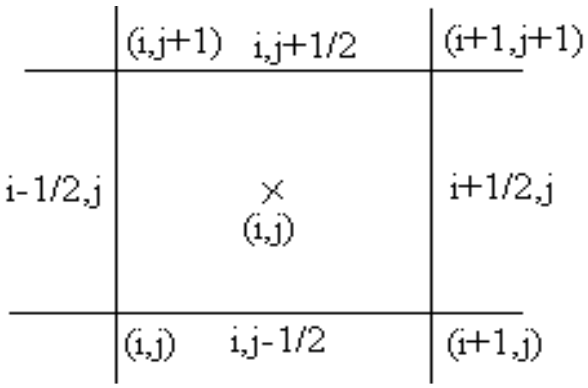

Figure 1. Computational cell.

The pressure at the face (i+½,j), related to the cell (i,j), is calculated by a similar formula:

$$p_{i+1/2,j} = p_L^+ + p_R^- , \tag{23}$$

with $p^{+/-}$ denoting the pressure separation and according to Van Leer (1982):

$$p^+ = \begin{cases} p, & \text{if } M \geq 1; \\ 0.25p(M+1)^2(2-M), & \text{if } |M| < 1 \\ 0, & \text{if } M \leq -1; \end{cases};$$

and

$$p^- = \begin{cases} 0, & \text{if } M \geq 1; \\ 0.25p(M-1)^2(2+M), & \text{if } |M| < 1 \\ p, & \text{if } M \leq -1. \end{cases}; \tag{24}$$

The definition of a dissipative term ϕ determines the particular formulation of the convective fluxes. The following choice corresponds to the Van Leer (1982) scheme, according to Radespiel and Kroll (1995):

$$\phi_{i+1/2,j} = \phi_{i+1/2,j}^{VL} = \begin{cases} |M_{i+1/2,j}|, \\ |M_{i+1/2,j}| + 0.5(M_R - 1)^2, \\ |M_{i+1/2,j}| + 0.5(M_L + 1)^2, \end{cases}$$

$$\text{if } |M_{i+1/2,j}| \geq 1;$$

$$\text{if } 0 \leq M_{i+1/2,j} < 1;$$

$$\text{if } -1 < M_{i+1/2,j} \leq 0. \tag{25}$$

The aforementioned equations clearly show that to a supersonic cell face Mach number, the Van Leer (1982) scheme represents a discretization purely upwind, using either the left state or the right state to the convective terms and to the pressure, depending on the Mach number signal. This Van Leer (1982) scheme is first order accurate in space. The time integration is performed using an explicit Runge-Kutta method of five stages, second order accurate, and can be represented in generalized form by:

$$Q_{i,j}^{(0)} = Q_{i,j}^{(n)}$$

$$Q_{i,j}^{(k)} = Q_{i,j}^{(0)} - \alpha_k \Delta t_{i,j} \left[R\left(Q_{i,j}^{(k-1)}\right) / V_{i,j} + G\left(Q_{i,j}^{(k-1)}\right) \right],$$

$$Q_{i,j}^{(n+1)} = Q_{i,j}^{(k)} \tag{26}$$

with k = 1,...,5; α_1 = 1/4, α_2 = 1/6, α_3 = 3/8, α_4 = 1/2 and α_5 = 1. The gradients of the primitive variables are calculated using the Green theorem, which considers that the gradient of a primitive variable is constant at the volume and that the volume integral which defines the gradient is replaced by a surface integral (Long et al., 1991). To the $\partial u/\partial x$ gradient, for example, it is possible to write:

$$\frac{\partial u}{\partial x} = \frac{1}{V}\int_V \frac{\partial u}{\partial x} dV = \frac{1}{V}\int_S u\left(\vec{n}_x \bullet d\vec{S}\right) =$$
$$\frac{1}{V}\int_{S_x} u dS_x \cong \frac{1}{V}\left[0.5\left(u_{i,j} + u_{i,j-1}\right)S_{x_{i,j-1/2}}\right.$$
$$+0.5\left(u_{i,j} + u_{i+1,j}\right)S_{x_{i+1/2,j}} +$$
$$0.5\left(u_{i,j} + u_{i,j+1}\right)S_{x_{i,i+1/2}}$$
$$\left. + 0.5\left(u_{i,j} + u_{i-1,j}\right)S_{x_{i-1/2,j}}\right]. \quad (27)$$

MUSCL APPROACH

Second order spatial accuracy can be achieved by introducing more upwind points or cells in the schemes. It has been noted that the projection stage, whereby the solution is projected in each cell face (i-1/2,j; i+1/2,j) on piecewise constant states, is the cause of the first order space accuracy of the Godunov schemes (Hirsch, 1990). Hence, it is sufficient to modify the first projection stage without modifying the Riemann solver, in order to generate higher spatial approximations. The state variables at the interfaces are thereby obtained from an extrapolation between neighboring cell averages. This method for the generation of second order upwind schemes based on variable extrapolation is often referred to in the literature as the MUSCL (Monotone Upstream-centered Schemes for Conservation Laws) approach. The use of nonlinear limiters in such procedure, with the intention of restricting the amplitude of the gradients appearing in the solution, avoiding thus the formation of new extrema, allows that first order upwind schemes be transformed in TVD high resolution schemes with the appropriate definition of such nonlinear limiters, assuring monotone preserving and total variation diminishing methods. Details of the present implementation of the MUSCL procedure are found in Maciel (2010). In this work, the minmod nonlinear limiter, defined in Hirsch (1990) and in Maciel (2010), was employed in the numerical simulations.

TURBULENCE MODELS

In this work, the k-ε turbulence model of Jones and Launder (1972) and the k-ω^2 model of Wilcox and Rubesin (1980) were studied.

Jones and Launder (1972) model

In the Jones and Launder (1972) turbulence model, s = ε. To define the turbulent viscosity, or eddy viscosity, it is necessary to define the turbulent Reynolds number:

$$\mathbf{Re}_T = k/\left(\nu_M \omega\right),$$

with

$$\nu_M = \mu_M/\rho$$

and

$$\omega = \varepsilon/k. \quad (28)$$

It is also necessary to determine the D damping factor:

$$D = e^{\left[-3.4/\left(1+0.02\,\mathbf{Re}_T\right)^2\right]}. \quad (29)$$

The turbulent viscosity is expressed in terms of k and ω as:

$$\mu_T = \mathbf{Re}\, C_\mu D\rho k/\omega, \quad (30)$$

with C_μ a constant to be defined.

The source term denoted by G in the governing equation contains the production and dissipation terms of k and ε. To the Jones and Launder (1972) model, the G_k and G_ε terms have the following expressions:

$$G_k = -P_k - D_k$$

and

$$G_\varepsilon = -P_\varepsilon - D_\varepsilon, \quad (31)$$

where:

$$P = \left(\frac{\partial u}{\partial y} + \frac{\partial v}{\partial x}\right)\frac{\partial u}{\partial y},\ P_k = \left(\frac{C_\mu DP}{\omega^2}\right)\rho\omega k \Big/ \mathbf{Re} \quad (32)$$

$$D_k = \left[-\frac{2}{3}\left(\frac{\partial u}{\partial x} + \frac{\partial v}{\partial y}\right)\Big/\omega - \left(1 + \frac{2\nu_M}{\varepsilon}\frac{\partial k}{\partial y}\right)\right]\rho\omega k \Big/ \mathbf{Re},$$

$$P_\varepsilon = \left(\frac{C_{\varepsilon 1} C_\mu DP}{\omega^2}\right)\rho\omega\varepsilon \Big/ \mathbf{Re}; \quad (33)$$

$$D_\varepsilon = \left[-\frac{2}{3} C_{\varepsilon 1} \left(\frac{\partial u}{\partial x} + \frac{\partial v}{\partial y} \right) \Big/ \omega + 2 C_\mu D \nu_M \left(\frac{\partial^2 u}{\partial y^2} \right)^2 \Big/ \omega^3 - C_{\varepsilon 2} E_f \right] \rho \omega \varepsilon \Big/ \mathbf{Re} \quad , \tag{34}$$

with the second damping factor E_f defined as: $E_f = 1 - 2/9\, e^{\left(-\mathbf{Re}_T^2/36\right)}$. The closure coefficients adopted to the Jones and Launder (1972) model assume the following values: $\sigma_k = 1.0$; $\sigma_\varepsilon = 1.3$; $C_\mu = 0.09$; $C_{\varepsilon 1} = 1.45$; $C_{\varepsilon 2} = 1.92$; Prd_L = 0.72; Prd_T = 0.9.

Wilcox and Rubesin (1980) model

In the Wilcox and Rubesin (1980) turbulence model, s $=\omega^2$. To define the turbulent viscosity, it is also necessary to define the turbulent Reynolds number, according to Equation (28), with ω defined as $\sqrt{s} = \sqrt{\omega^2}$. It needs to define a D damping factor:

$$D = 1 - \alpha e^{\left(-\mathbf{Re}_T\right)}, \quad \text{with: } \alpha \text{ a constant to be defined.} \tag{35}$$

The turbulent viscosity is expressed in terms of k and ω as:

$$\mu_T = \mathbf{Re}\, D \rho k / \omega . \tag{36}$$

The source term denoted by G in the governing equation contains the production and dissipation terms of k and ω^2. To the Wilcox and Rubesin (1980) model, the G_k and G_{ω^2} terms have the following expressions:

$$G_k = -P_k - D_k$$

and

$$G_{\omega^2} = -P_{\omega^2} - D_{\omega^2}, \tag{37}$$

where:

$$P = \left(\frac{\partial u}{\partial y} + \frac{\partial v}{\partial x} \right) \frac{\partial u}{\partial y}, \qquad P_k = \left(\frac{DP}{\omega^2} \right) \rho \omega k \Big/ \mathbf{Re},$$

$$D_k = \left[-\frac{2}{3} \left(\frac{\partial u}{\partial x} + \frac{\partial v}{\partial y} \right) \Big/ \omega - \beta^* \right] \rho \omega k \Big/ \mathbf{Re}; \tag{38}$$

$$P_{\omega^2} = \left(\frac{\gamma_\infty EP}{\omega^2} \right) \rho \omega^3 \Big/ \mathbf{Re},$$

$$D_{\omega^2} = \left\{ -\frac{2}{3} \gamma_\infty \left(\frac{\partial u}{\partial x} + \frac{\partial v}{\partial y} \right) \Big/ \omega - \left[\beta + \frac{2}{\sigma_{\omega^2}} \left(\frac{\partial \sqrt{k/\omega^2}}{\partial y} \right)^2 \right] \right\} \rho \omega^3 \Big/ \mathbf{Re}, \tag{39}$$

with the second damping factor E defined as: $E = 1 - \alpha e^{\left(-0.5\, \mathbf{Re}_T\right)}$. The closure coefficients adopted to the Wilcox and Rubesin (1980) model assume the following values: $\alpha = 0.99174; \beta = 0.15; \beta^* = 0.09$; $\sigma_k = 2.0$; $\sigma_{\omega^2} = 2.0$; $\gamma_\infty = 0.9$; Prd_L = 0.72; Prd_T = 0.9.

INITIAL AND BOUNDARY CONDITIONS

Initial condition

k-ε model

Freestream values, at all grid cells, are adopted for all flow properties as initial condition, as suggested by Jameson and Mavriplis (1986) and Maciel (2002). Therefore, the vector of conserved variables is defined as:

$$Q_{i,j} = \left\{ 1 \quad M_\infty \cos\alpha \quad M_\infty \sin\alpha \quad \frac{1}{\gamma(\gamma-1)} + 0.5 M_\infty^2 \quad f_1 K \quad f_2 K \right\}^t, \tag{40}$$

where α is the angle of attack, K is the kinetic energy of the mean flow and f_1 and f_2 are fractions. The kinetic energy of the mean flow is determined, considering the present nondimensionalization, as $K = 0.5 M_\infty^2$. The values adopted for f_1 and f_2 in the present work were 0.005 and 0.2, respectively.

k-ω² model

Again freestream values, at all grid cells, are adopted for all flow properties as initial condition, as suggested by

Jameson and Mavriplis (1986) and Maciel (2002). Therefore, the vector of conserved variables is defined as:

$$Q_{i,j} = \left\{ 1 \quad M_\infty \cos\alpha \quad M_\infty \sin\alpha \quad \frac{1}{\gamma(\gamma-1)} + 0.5M_\infty^2 \quad k_\infty \quad \omega_\infty^2 \right\}^t , \tag{41}$$

where k_∞ is the freestream turbulent kinetic energy and ω_∞ is the freestream turbulent vorticity. These parameters assumes the following values in the present work: k_∞ = 1.0 × 10^{-6} and $\omega_\infty = (10u_\infty / l_{REF})^2$, with u_∞ the freestream u Cartesian component and l_{REF} a characteristic length, the same adopted in the definition of the Reynolds number.

Boundary conditions

The boundary conditions are basically of four types: Solid wall, entrance, exit and far field. These conditions are implemented with the help of ghost cells. Wall condition: At a solid boundary, the non-slip condition is enforced. Therefore, the tangent velocity component of the ghost volume at wall has the same magnitude as the respective velocity component of its real neighbor cell, but opposite signal. In the same way, the normal velocity component of the ghost volume at wall is equal in value, but opposite in signal, to the respective velocity component of its real neighbor cell.

The normal pressure gradient of the fluid at the wall is assumed to be equal to zero in a boundary-layer like condition. The same hypothesis is applied for the normal temperature gradient at the wall, assuming an adiabatic wall. The normal gradient of the turbulence kinetic energy at the wall is also assumed to be equal to zero.

k-ε model

From the aforementioned considerations, density, pressure and turbulence kinetic energy at the ghost volume are extrapolated from the respective values of its real neighbor volume (zero order extrapolation). The total energy is obtained by the perfect gas law and the rate of dissipation of the turbulence kinetic energy is determined by the following expression, considering production-destruction equilibrium:

$$(\rho\varepsilon)_{ghost} = C_\mu^{3/4} k_w^{3/2} / (0.41 d_n), \tag{42}$$

where k_w is the wall turbulence kinetic energy and d_n is the distance of the first mesh point to the wall.

The properties of the first real volumes (j = 1) are necessary to be determined, aiming to guarantee that the u profile is correctly calculated by the numerical scheme. The u component of these cells is determined by the "wall law". It is initially necessary to calculate the wall shear stress, which is defined as:

$$\tau_w = \rho u C_\mu^{0.25} k_w^{0.5} / u^+ , \tag{43}$$

where u^+ is defined as:

$$u^+ = d^+, \quad d^+ < 5; \qquad u^+ = -3.05 + 5\ln d^+, \quad 5 \le d^+ < 30;$$
$$u^+ = 5.5 + 2.5\ln d^+, \quad 30 \le d^+ < 200, \tag{44}$$

with $d^+ = \rho C_\mu^{0.25} k_w^{0.5} d_n / \mu_M$. The value of u of the real volume at the wall is obtained from:

$$u = d_n \tau_w / \mu_M + u_{ghost} \tag{45}$$

The v component is extrapolated from the ghost volume, with opposite signal, and the pressure is extrapolated from the real volume at j = 2. The turbulence kinetic energy is defined by its value at wall and the total energy of this volume is determined by the state equation for a perfect gas. The rate of dissipation of the turbulence kinetic energy to this volume is determined by Equation (46).

k-ω² model

From the aforementioned considerations, density and pressure are extrapolated from the respective values of its real neighbor volume (zero order extrapolation). The total energy is obtained by the state equation for a perfect gas. The turbulent kinetic energy and the turbulent vorticity at the ghost volumes are determined by the following expressions:

$$k_{ghost} = 0.0$$

and

$$\omega_{ghost} = \left[(38/3\nu_M) / (\beta d_n^2) \right]^2 , \tag{46}$$

where β assumes the value 3/40 and d_n is the distance of the first mesh point to the wall.

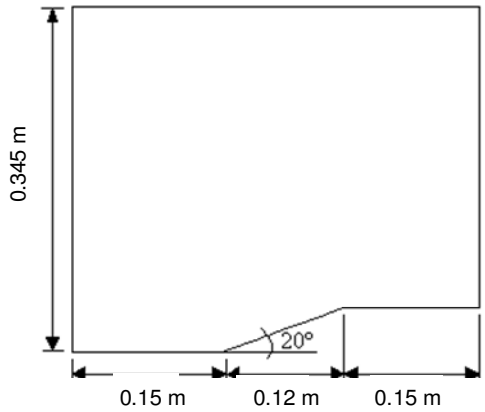

Figure 2. Ramp configuration.

Entrance condition

Subsonic flow

Five properties are specified and one extrapolated. This approach is based on information propagation analysis along characteristic directions in the calculation domain (Maciel, 2002). In other words, for subsonic flow, five characteristic propagate information point into the computational domain. Thus five flow properties must be fixed at the inlet plane. Just one characteristic line allows information to travel upstream. So, one flow variable must be extrapolated from the grid interior to the inlet boundary. The pressure was the extrapolated variable from the real neighbor volumes, for all studied problems. Density and velocity components adopted values of freestream flow. The turbulence kinetic energy and the rate of dissipation of the turbulence kinetic energy were fixed with the values of the initial condition, with the modification of $K = 0.5u^2$. To the k-ω^2 model, the turbulence kinetic energy and the turbulence vorticity assume the values of the initial condition (freestream flow). The total energy is determined by the state equation of a perfect gas.

Supersonic flow

In this case, no information travels upstream; therefore all variables are fixed with their of freestream values.

Exit condition

Subsonic flow

Five characteristic propagate information outward the computational domain. Hence, the associated variables should be extrapolated from interior information. The characteristic direction associated to the "(q_{normal}-a)" velocity should be specified because it point inward to the computational domain (Maciel, 2002). In this case, the ghost volume pressure is specified from its initial value. Density, velocity components, the turbulence kinetic energy, the rate of dissipation of the turbulence kinetic energy and the turbulence vorticity are extrapolated. The total energy is obtained from the state equation of a perfect gas.

Supersonic flow

All variables are extrapolated from interior grid cells, as no flow information can make its way upstream. In other words, nothing can be fixed.

Far field condition

To both problems and only to the k-ω^2 model, the mean flow kinetic energy is assumed to be $K = 0.5u^2$ and the turbulence kinetic energy at the far field adopts the value k_{ff} = 0.01K, or 1% of K. The turbulence vorticity is determined by its freestream value.

RESULTS

Tests were performed in an INTEL CELERON - 1.5 GHz and 1.0 Gbytes of RAM microcomputer. Three orders of reduction of the maximum residual in the field were considered to obtain a converged solution. The residual was defined as the value of the discretized conservation equation. The entrance or attack angle was adopted equal to zero. The ratio of specific heats, γ, assumed the value 1.4.

Ramp physical problem

Figure 2 exhibits the ramp configuration. An algebraic mesh of 61 × 70 points, with an exponential stretching of 10% in the η direction was used. This mesh is equivalent in finite volumes as being composed of 4,140 rectangular cells and 4,270 nodes. This mesh is shown in Figure 3. The initial condition adopted a freestream Mach number of 2.0, at a flight altitude of 10,000 m, a characteristic configuration length equals to 0.041 m and a corresponding Reynolds number of 6.966×10^5, based on Fox and McDonald (1988). The Courant-Friedrichs-Lewy (CFL) number to the laminar and turbulent simulations was 0.1.

Figure 4 shows the pressure contours obtained by the Van Leer (1982) scheme in the laminar case. Figures 5 and 6 exhibit the pressure contours obtained by the Jones and Launder (1972) and the Wilcox and Rubesin

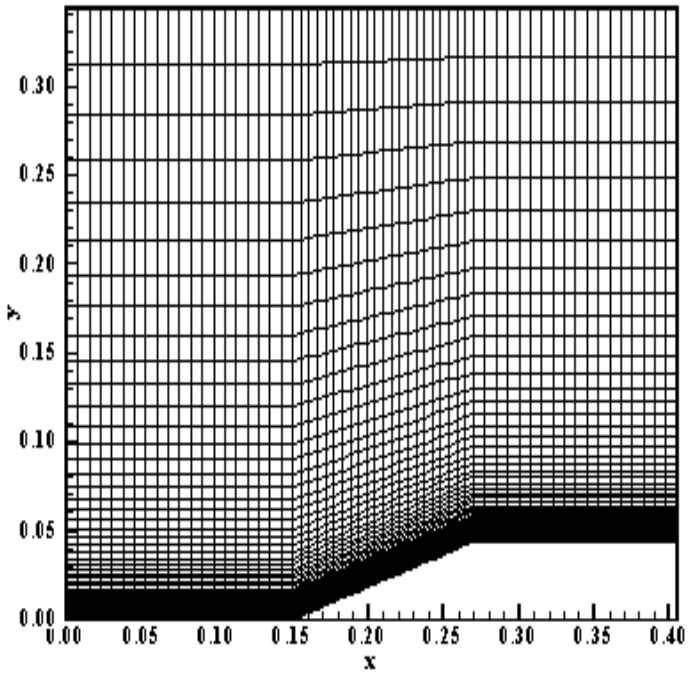

Figure 3. Ramp mesh.

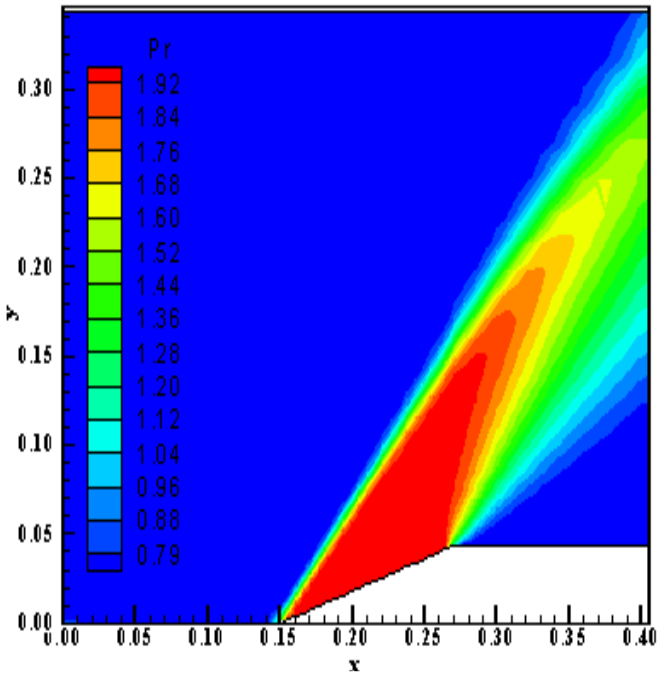

Figure 5. Pressure contours (JL).

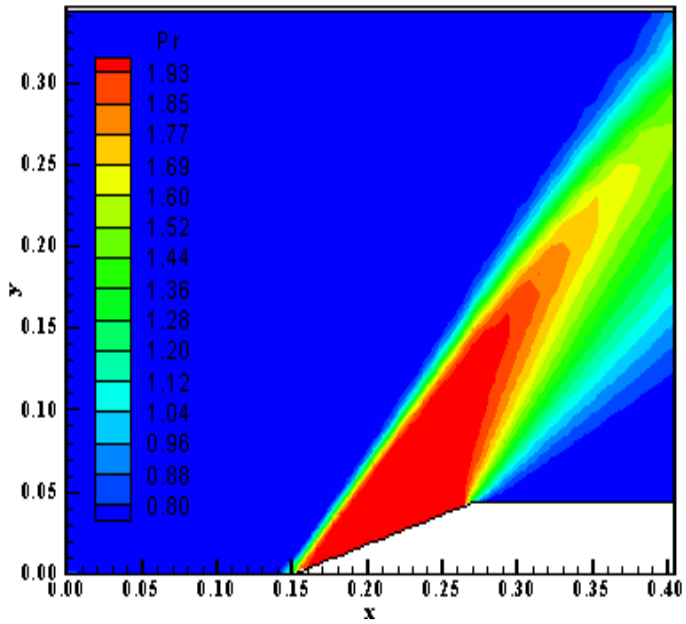

Figure 4. Pressure contours (Lam).

(1980) turbulence models, respectively. As can be observed, the most severe pressure field is obtained by the Van Leer (1982) scheme using the Wilcox and Rubesin (1980) turbulence model.

Figure 7 shows the Mach number contours obtained by the Van Leer (1982) scheme in the laminar case. Figures 8 and 9 exhibit the Mach number contours obtained by the Jones and Launder (1972) and the Wilcox and Rubesin (1980) turbulence models, respectively.

As can be observed, the most intense Mach number field is obtained by the Van Leer (1982) scheme using the Jones and Launder (1972) turbulence model.

Figure 10 shows the laminar and turbulent wall pressure distributions obtained by the Van Leer (1982) scheme. They are compared with the inviscid solution, which corresponds to the correct solution according to the boundary layer theory. The laminar and the turbulence model of Jones and Launder presents the same pressure plateau width, whereas the Wilcox and Rubesin (1980) presents smaller pressure plateau width. However, the formers slightly under-predict the pressure plateau, whereas the latter estimates the correct value to this plateau. Moreover, the Wilcox and Rubesin (1980) model predicts a discrete separation before the ramp. All solutions, laminar and turbulent, predict the same value to the expansion pressure after the ramp. They agree correctly with the inviscid solution.

One way to quantitatively verify if the solutions are generated by each case (laminar and turbulent) is by determining the shock angle of the oblique shock wave, β, measured in relation to the initial direction of the flow field. Anderson (1984: 352-353) presents a diagram with values of the shock angle, β, to oblique shock waves. The value of this angle is determined as function of the freestream Mach number and of the deflection angle of the flow after the shock wave, ϕ. To the ramp problem, ϕ = 20º (ramp inclination angle) and the freestream Mach

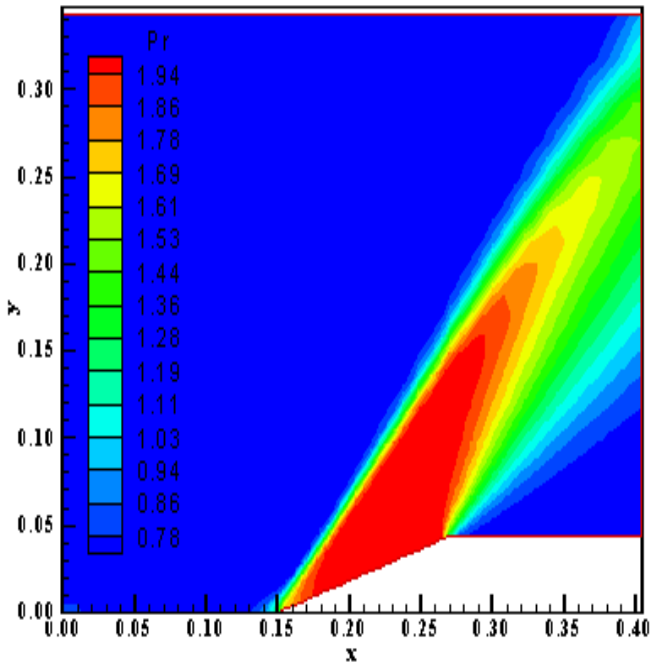

Figure 6. Pressure contours (WR).

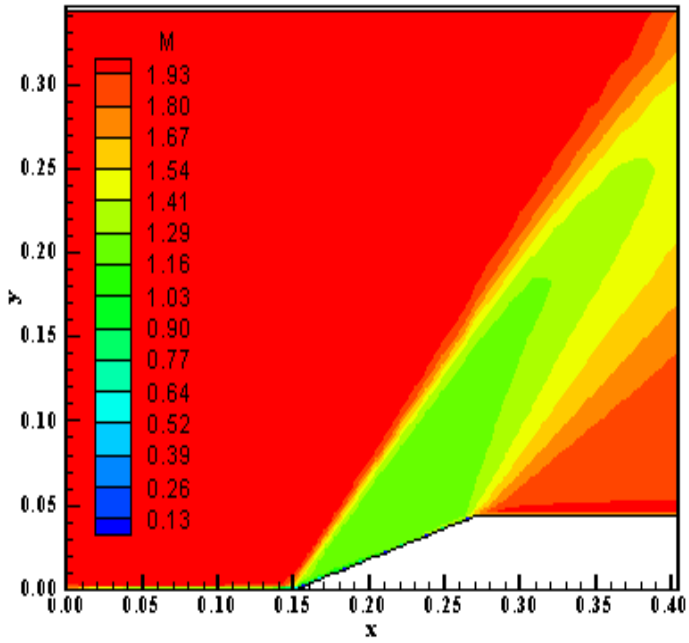

Figure 7. Mach number contours (Lam).

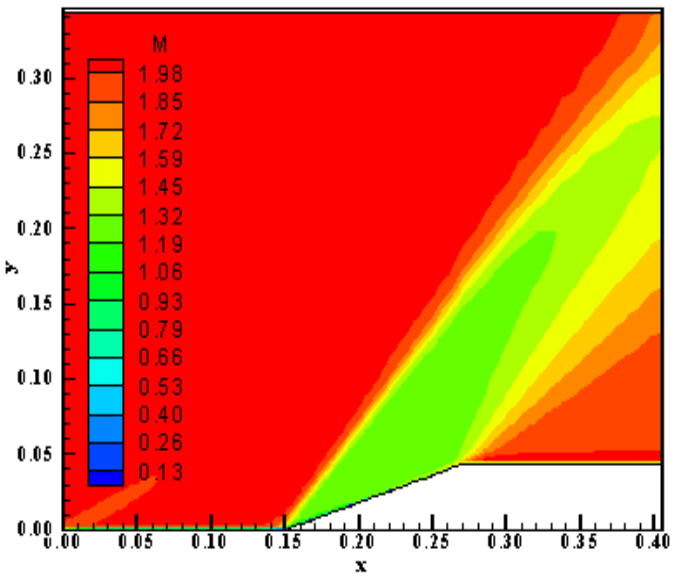

Figure 8. Mach number contours (JL).

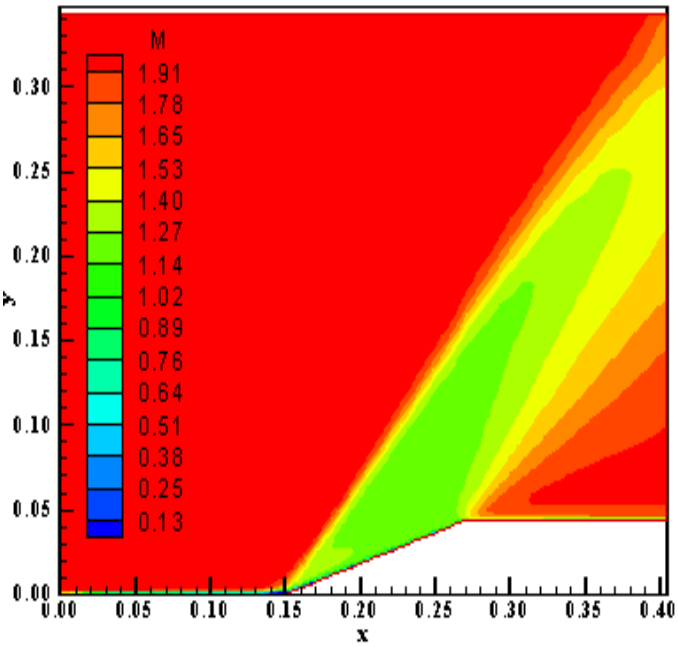

Figure 9. Mach number contours (WR).

number is 2.0, resulting from this diagram a value to β equals to 53.0º. Using a transfer in Figures 4 to 6, it is possible to obtain the shock angle, β, as well as the respective percentage errors, presented in Table 2. The best result was due to the Wilcox and Rubesin (1980) turbulence model, which predicts correctly the shock angle (error of 0.00%).

Blunt body physical problem

Figure 11 exhibits the blunt body configuration. An algebraic mesh of 103 × 70 points, with an exponential stretching of 10% in the η direction was used. This mesh is equivalent in finite volumes as being composed of 7,038 rectangular cells and 7,210 nodes. This mesh is shown in Figure 12. The initial condition adopted a freestream Mach number of 3.0, at a flight altitude of

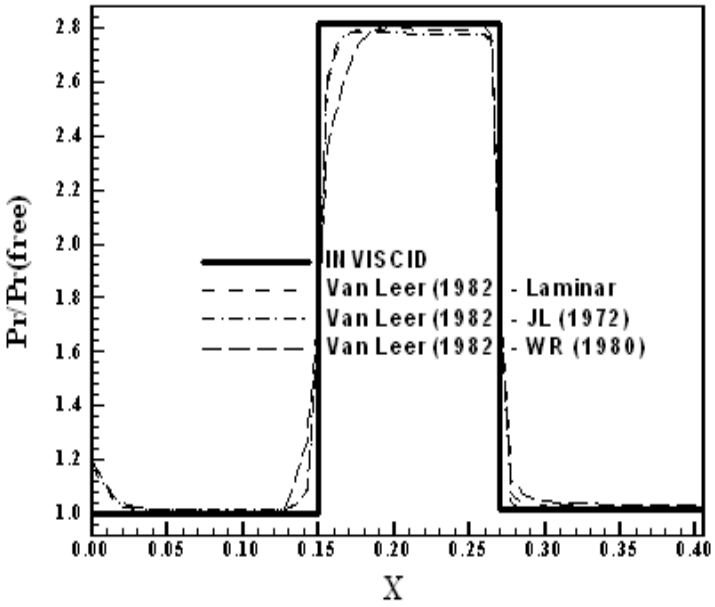

Figure 10. Wall pressure distributions.

Table 2. Values of the shock angle of the oblique shock wave and respective percentage errors.

Type of viscous case	β(°)	Error (%)
Laminar	53.4	0.75
Jones and Launder (1972) - turbulent	52.9	0.19
Wilcox and Rubesin (1980) - turbulent	53.0	0.00

40,000 m, a characteristic configuration length equals to 3.76 m and a corresponding Reynolds number of 8.933×10^5 (Fox and McDonald, 1988). The CFL number to the laminar and turbulent simulations was 0.1.

Figure 13 shows the pressure contours obtained by the Van Leer (1982) scheme in the laminar case. Figures 14 and 15 exhibit the pressure contours obtained by the Jones and Launder (1972) and the Wilcox and Rubesin (1980) turbulence models, respectively. As can be observed, the most severe pressure field is obtained by the Van Leer (1982) scheme using the Wilcox and Rubesin (1980) turbulence model.

Figure 16 shows the Mach number contours obtained by the Van Leer (1982) scheme in the laminar case. Figures 17 and 18 exhibit the Mach number contours obtained by the Jones and Launder (1972) and the Wilcox and Rubesin (1980) turbulence models, respectively. As can be observed, the most intense Mach number field is obtained by the Van Leer (1982) scheme using the Wilcox and Rubesin (1980) turbulence model.

Figure 19 shows the –Cp distribution of the Van Leer (1982) scheme in the laminar and turbulent cases. As can be observed, the Jones and Launder (1972) turbulence model slightly under-predicts the –Cp plateau. The Wilcox and Rubesin (1980) turbulence model agrees with the laminar solution.

Table 3 shows the lift and drag aerodynamic coefficients calculated by the Van Leer (1982) scheme in the laminar and turbulent cases. As the geometry is symmetrical and an attack angle of zero value was adopted in the simulations, the lift coefficient should have a zero value. The most correct value to the lift coefficient is due to the laminar simulation, but the Wilcox and Rubesin (1980) turbulence model provides the second best value to this coefficient.

Another possibility to quantitative comparison of the laminar and turbulent cases is the determination of the stagnation pressure ahead of the configuration. Anderson (1984) presents a table of normal shock wave properties in its B Appendix. This table permits the determination of some shock wave properties as function of the freestream Mach number. In front of the blunt body configuration, the shock wave presents a normal shock behavior, which permits the determination of the stagnation pressure, behind the shock wave, from the tables encountered in Anderson (1984). So it is possible

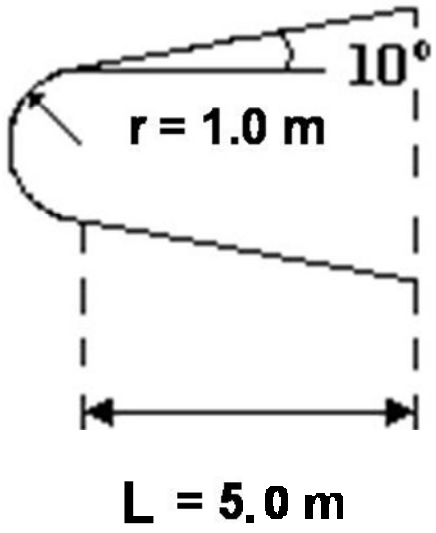

Figure 11. Blunt body configuration.

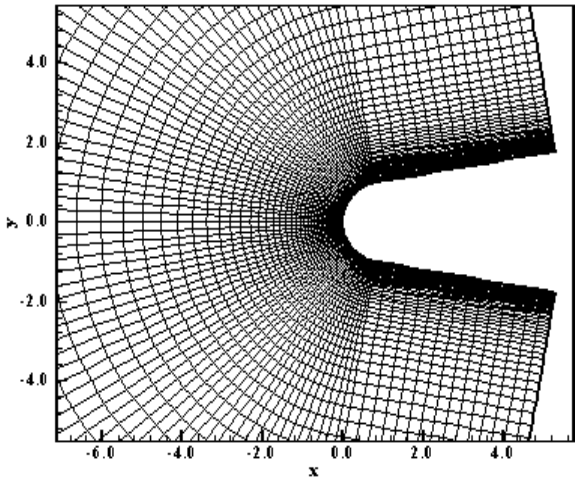

Figure 12. Blunt body mesh.

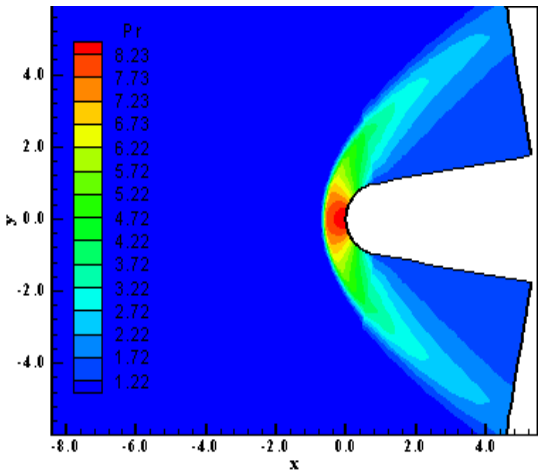

Figure 13. Pressure contours (Lam).

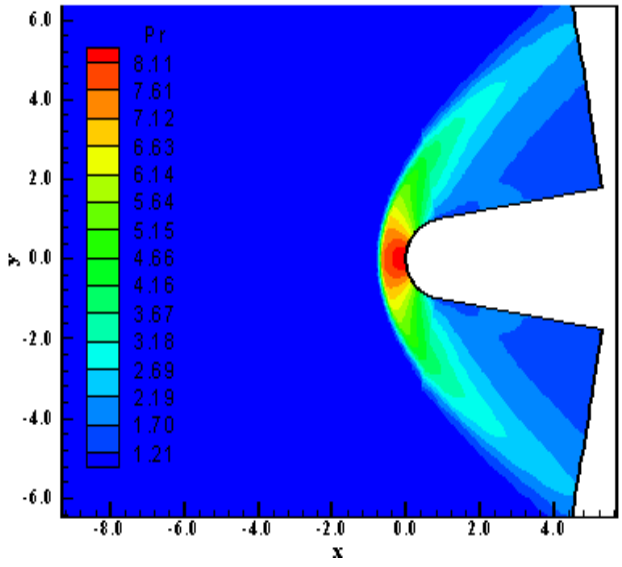

Figure 14. Pressure contours (JL).

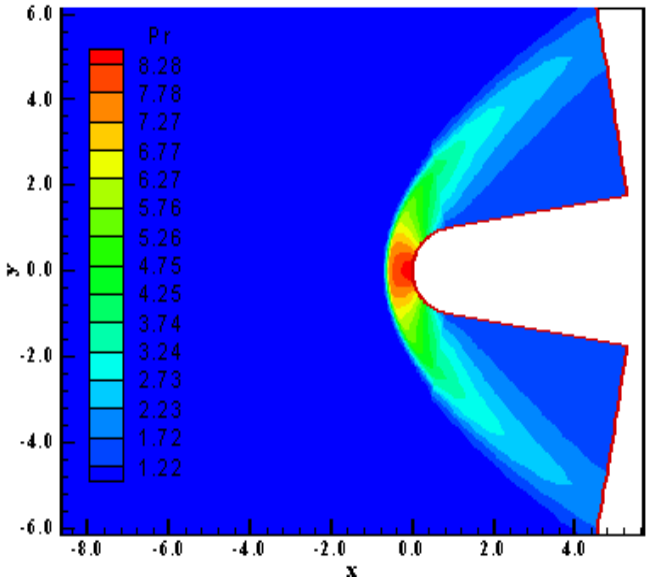

Figure 15. Pressure contours (WR).

to determine the ratio pr_0/pr_∞ from Anderson (1984), where pr_0 is the stagnation pressure in front of the configuration and pr_∞ is the freestream pressure (equals to $1/\gamma$ to the present nondimensionalization).

Hence, to this problem, M_∞ = 3.0 corresponds to pr_0/pr_∞ = 12.06 and remembering that pr_∞ = 0.714, it is possible to conclude that pr_0 = 8.61. Values of the stagnation pressure to the laminar and turbulent cases and respective percentage errors are shown in Table 4. They are obtained from Figures 13 to 15. As can be observed, the Wilcox and Rubesin (1980) turbulence

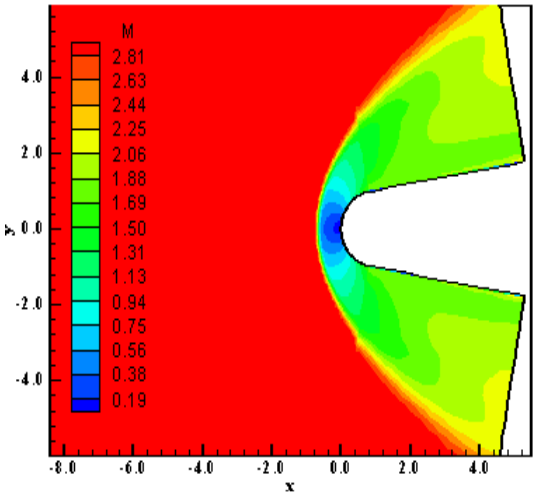

Figure 16. Mach number contours (Lam).

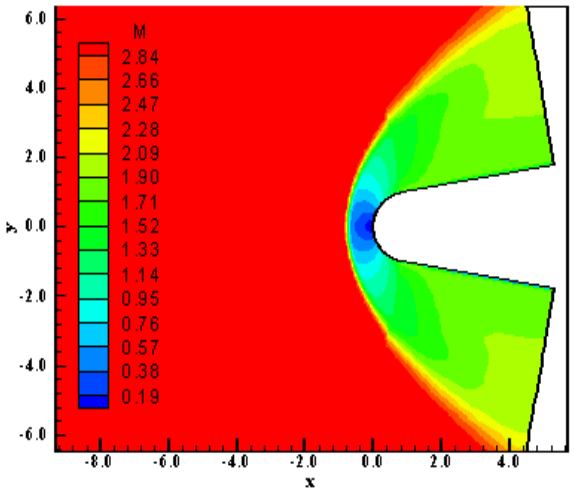

Figure 17. Mach number contours (JL).

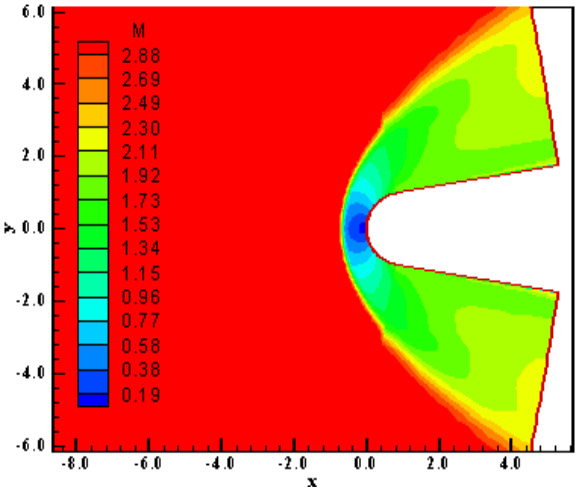

Figure 18. Mach number contours (WR).

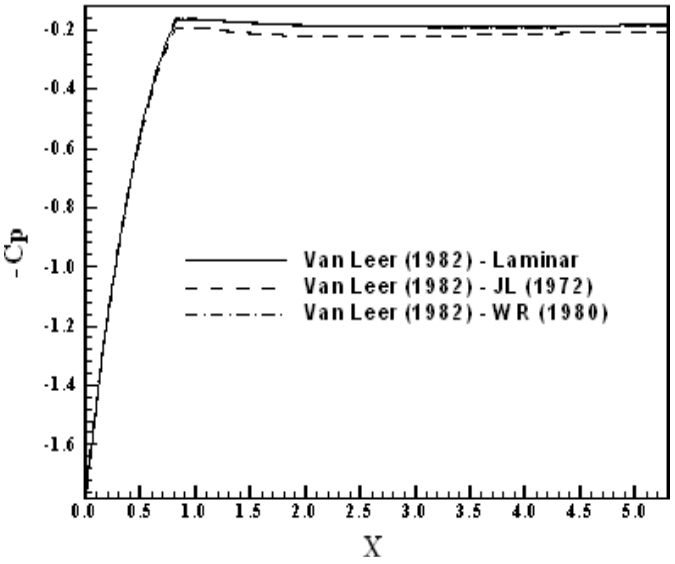

Figure 19. -Cp distributions.

model presents the best result, with a percentage error of 3.83%.

The computational costs to each case are: Laminar - 0.0001520 seconds/per cell/per iteration; Jones and Launder (1972) - 0.0001766 seconds/per cell/per iteration; and Wilcox and Rubesin (1980) - 0.0001803 seconds/per cell/per iteration. The Jones and Launder (1972) model is roughly 2.10% cheaper than the Wilcox and Rubesin (1980) model.

CONCLUSIONS

In the present work, the Van Leer (1982) flux vector splitting scheme is implemented, on a finite-volume context. The 2-D Favre-averaged Navier-Stokes equations are solved using an upwind discretization on a structured mesh. The Jones and Launder (1972) k-ε and the Wilcox and Rubesin (1980) k-ω^2 two-equation models are used in order to close the problem. The physical problems under studies are the low supersonic flow along a ramp and the moderate supersonic flow around a blunt body configuration. The implemented scheme uses a MUSCL procedure to reach second order accuracy in space. The time integration uses a Runge-Kutta method of five stages and is second order accurate. The algorithm is accelerated to the steady state solution using a spatially variable time step. This technique has proved excellent gains in terms of convergence rate as reported in Maciel (2005, 2008).

The results have demonstrated that the Wilcox and Rubesin (1980) model has yielded more critical pressure fields than the ones due to Jones and Launder (1972). The shock angle of the oblique shock wave in the ramp problem and the stagnation pressure ahead of the blunt

Table 3. Lift and drag aerodynamic coefficients- laminar and turbulent cases.

Type of viscous case	c_L	c_D
Laminar	-4.104×10^{-15}	0.507
Jones and Launder (1972) - turbulent	1.192×10^{-10}	0.515
Wilcox and Rubesin (1980) - turbulent	3.897×10^{-12}	0.510

Table 4. Values of the stagnation pressure and respective percentage errors.

Type of viscous case	pr_0	Error (%)
Laminar	8.23	4.41
Jones and Launder (1972) - turbulent	8.11	5.81
Wilcox and Rubesin (1980) - turbulent	8.28	3.83

body configuration are better predicted by the Wilcox and Rubesin (1980) turbulence model. In the ramp problem, the best wall pressure distributions are due to the laminar and the Jones and Launder (1972) turbulence model because they provide the correct pressure plateau width. However, they slightly under-predicted the pressure plateau. The Wilcox and Rubesin (1980) turbulence model predicted the correct pressure plateau. The shock angle of the oblique shock wave is correctly predicted by the Wilcox and Rubesin (1980) turbulence model. In the blunt body case, the –Cp distribution generated by the Wilcox and Rubesin (1980) model is in agreement with that generated by the laminar solution. The lift aerodynamic coefficient is better predicted by the laminar solution, although the second best solution is provided by the Wilcox and Rubesin (1980) model. The stagnation pressure ahead of the configuration is best predicted by the latter, with an error of 3.83%. The Jones and Launder (1972) turbulence model is roughly 2.10% cheaper than the Wilcox and Rubesin (1980) turbulence model, which is insignificant. Hence, the Wilcox and Rubesin (1980) is the best turbulence model in this study.

REFERENCES

Anderson Jr, JD (1984). Fundamentals of Aerodynamics, McGraw-Hill, Inc., EUA, p. 563.

Baldwin BS, Lomax H (1978). Thin Layer Approximation and Algebraic Model for Separated Turbulent Flows. AIAA, pp. 78-257.

Cebeci T, Smith AMO (1970). A Finite-Difference Method for Calculating CompressibleLaminar and Turbulent Boundary Layers. J. Basic. Eng. Trans. ASME, Ser. B, 92 (3): 523-535.

Fox RW, McDonald AT (1988). *Introdução à Mecânica dos Fluidos*, Ed. Guanabara Koogan, Rio de Janeiro, RJ, Brazil, p. 632.

Harten A (1983). High Resolution Schemes for Hyperbolic Conservation Laws. J. Comput. Phy., 49: 357-393.

Hirsch C (1990). Numerical Computation of Internal and External Flows – Computational Methods for Inviscid and Viscous Flows, John Wiley & Sons Ltd, p. 691.

Jacon F, Knight D (1994). A Navier-Stokes Algorithm for Turbulent Flows Using an Unstructured Grid and Flux Difference Splitting. AIAA, pp. 94-2292.

Jameson A, Mavriplis D (1986). Finite Volume Solution of the Two-Dimensional Euler Equations on a Regular Triangular Mesh. AIAA J., 24 (4): 611-618.

Jameson A, Schmidt W, Turkel E (1981). Numerical Solution of the Euler Equations by Finite Volume Methods Using Runge-Kutta Time Stepping Schemes. AIAA, pp. 81-1259.

Jones WP, Launder BE (1972). The Prediction of Laminarization with a Two-Equation Model of Turbulence. Int. J. Heat. Mass. Transfer, 15: 301-304.

Kergaravat Y, Knight D (1996). A Fully Implicit Navier-Stokes Algorithm for Unstructured Grids Incorporating a Two-Equation Turbulence Model. AIAA, pp. 96-0414.

Kutler P (1975). Computation of Three-Dimensional, Inviscid Supersonic Flows. Lecture Notes Phys., 41: 287-374.

Liou M, Steffen Jr, CJ (1993). A New Flux Splitting Scheme. J. Comput. Phy., 107: 23-39.

Long LN, Khan MMS, Sharp HT (1991). Massively Parallel Three-Dimensional Euler/ Navier-Stokes Method. AIAA J., 29(5): 657-666.

MacCormack RW (1969). The Effect of Viscosity in Hypervelocity Impact Cratering. AIAA, pp. 69-354.

Maciel ESG (2002). Simulação Numérica de Escoamentos Supersônicos e Hipersônicos Utilizando Técnicas de Dinâmica dos Fluidos Computacional. Doctoral Thesis, ITA, CTA São José dos Campos, SP, Brazil.

Maciel ESG (2005). Analysis of Convergence Acceleration Techniques Used in Unstructured Algorithms in the Solution of Aeronautical Problems – Part I. Proceedings of the 18, International Congress of Mechanical Engineering (18I COBEM), Ouro Preto, MG, Brazil.

Maciel ESG (2008). Analysis of Convergence Acceleration Techniques Used in Unstructured Algorithms in the Solution of Aerospace Problems – Part II. Proceedings of the 12, Brazilian Congress of Thermal Engineering and Sciences (12 ENCIT), Belo Horizonte, MG, Brazil.

Maciel ESG (2010). Extension of the Steger and Warming and Radespiel and Kroll Algorithms to Second Order Accuracy and Implicit Formulation Applied to the Euler Equations in Two-Dimensions – Theory. Proceedings of the 6 National Congress of Mechanical Engineering (6 CONEM), Campina Grande, PB, Brazil.

Maciel ESG, Fico Jr NGCR (2004). Estudos de Escoamentos Turbulentos Utilizando o Modelo de Baldwin e Lomax e Comparação entre Algoritmos Explícitos e Implícitos. Proceedings of the III National Congress of Mechanical Engineering (3 CONEM), Belém, PA, Brazil.

Maciel ESG, Fico Jr, NGC R (2006). High Resolution Algorithms Coupled with Three Turbulence Models Applied to an Aerospace Flow Problem – Part I. AIAA, pp. 06-0292.

Maciel ESG, Fico Jr, NGC R (2008). Comparação Entre Modelos de Turbulência de Duas Equações Aplicados a um Problema Aeroespacial. *Proceedings of the Primer Congreso Argentino de Ingeniería Mecánica (I CAIM),* Bahía Blanca, Argentina.

Mavriplis DJ, Jameson A (1990). Multigrid Solution of the Navier-Stokes Equations onTriangular Meshes. AIAA J., 28(8): 1415-1425.

Pulliam TH, Chaussee DS (1981). A Diagonal Form of an Implicit

Approximate-Factorization Algorithm. J. Comput. Phy., 39: 347-363.
Radespiel R, Kroll N (1995). Accurate Flux Vector Splitting for Shocks and Shear Layers. J. Comput. Phy., 121: 66-78.
Sparlat PR, Allmaras SR (1992).. A One-Equation Turbulence Model for Aerodynamic Flows. AIAA, 92: 0439.
Van Leer B (1982). Flux-Vector Splitting for the Euler Equations. Proceedings of the 8th International Conference on Numerical Methods in Fluid Dynamics, E. Krause, Editor. Springer-Verlag, Berlin, Lecture Notes Phys., 170: 507-512.
Wilcox DC, Rubesin MW (1980). Progress in Turbulence Modeling for Complex Flow Fields Including the Effects of Compressibility. NASA TP-1517.